Niobium−Carbon Functionalities Supported by *meso*-Octaethylporphyrinogen and Derived Macrocycles

Sylviane Isoz and Carlo Floriani*

Institut de Chimie Minérale et Analytique, BCH, Université de Lausanne, CH-1015 Lausanne, Switzerland

Kurt Schenk

Section de Physique, Université de Lausanne, CH-1015 Lausanne, Switzerland

Angiola Chiesi-Villa and Corrado Rizzoli

Dipartimento di Chimica, Università di Parma, I-43100 Parma, Italy

Received July 12, 1995[⊗]

This report concerns the organometallic chemistry of niobium based on a macrocyclic ligand. To this purpose, the (*meso*-octaalkylporphyrinogen)niobium(V) complex [(η^5:η^1:η^5:η^1-Et_8N_4)-NbCl], **2**, has been used as an appropriate starting material. The ionization of the Nb−Cl bond by the use of $AgSO_3CF_3$ gave a bifunctional acid−base system with an increased acidity of the metal center in [(η^5:η^1:η^1:η^1-Et_8N_4)Nb(THF)(O_3SCF_3)], **3**. The alkylation of **2** with LiMe gave a quite stable Nb(V) organometallic derivative [(η^5:η^1:η^1:η^1-Et_8N_4)Nb−Me], **4**, which undergoes a migratory insertion reaction with Bu^{t}NC leading to an η^2-iminoacyl derivative [(η^5:η^1:η^1:η^1-Et_8N_4)Nb(Bu^{t}NC)(η^2-C(Me)=NBu^t)], **6** ($\nu_{C=N}$, 2217 and 1736 cm^{-1}). Two steps of the reaction have been identified. An attempt to functionalize the Nb=O in [(η^5:η^1:η^1:η^1-$Et_8(C_4H_2N)_3$(*p*-MeC_5H_2N)Nb=O], **7**, by the use of LiMe led, on the contrary, to [(η^1:η^1:η^1:η^1-Et_7(CH-Me)$(C_4H_2N)_3$(*p*-MeC_5H_2N)NbOLi$(THF)_3$], derived from the metalation of one of the *meso*-ethyl groups in **9**. While X-ray analysis provided information on the solid state structures of **3**, **4**, **6**, and **9**, NMR studies allowed us to establish a relationship between the bonding mode of the porphyrinogen in the solid state and in solution.

Introduction

Although niobium has an extremely rich and versatile organometallic chemistry, this is almost exclusively based on cyclopentadienyl, alkoxo, and amido ancillary ligands.[1] The use of macrocyclic type ligands, however, has a more recent and limited development[2] mainly due to the lack of appropriate starting materials.[3,4] Among them we should mention, however, the *trans*-[Cl_2Nb-(acacen)] [acacen = *N*,*N*′-ethylenebis(salicylideniminato) dianion] and the *cis*-[Cl_2Nb(tmtaa)] [tmtaa = dibenzotetramethyltetraazaannulene dianion].[4] Recently we have developed significant aspects of organometallic methodologies on zirconium[5] and, to a lesser extent, on other early transition metals[6] using the *meso*-octaethylporphyrinogen tetraanion(**I**) as the ancillary ligand.[7]

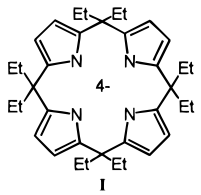

I

Some of the most interesting characteristics of this tetraanion include (i) the ligand binding mode, which can vary according to the electron needs of the metal along the reaction pathway.[5] In fact, each pyrrolyl anion can bind η^5, η^3, or η^1 providing 6, 4, or 2 electrons,

* To whom correspondence should be addressed.

[⊗] Abstract published in *Advance ACS Abstracts,* November 15, 1995.

(1) Labinger, J. A. In *Comprehensive Organometallic Chemistry*; Wilkinson, G., Stone, F. G. A., Abel, E. W., Eds.; Pergamon: London, 1982; Vol. 3, Chapter 25, p 705. Schrock, R. R.; Parshall, G. W. *Chem. Rev.* **1976**, *76*, 143. Wailes, P. C. *J. Organomet. Chem.* **1976**, *119*, 243. Labinger, J. A. *J. Organomet. Chem.* **1980**, *197*, 61. Labinger, J. A. *J. Organomet. Chem.* **1982**, *227*, 359. Yu, J. S.; Fanwick, P. E.; Rothwell, I. P. *J. Am. Chem. Soc.* **1990**, *112*, 8171. Bishop, P. T.; Dilworth, J. R.; Nicholson, T.; Zubieta, J. A. *J. Chem. Soc., Chem. Commun.* **1986**, 1123. Steffey, R. D.; Chamberlain, L. R.; Chesnut, R. W.; Chebi, D. E.; Fanwick, P.; Rothwell, I. P. *Organometallics* **1989**, *8*, 1419. Chamberlain, L. R.; Kerschner, J. L.; Rothwell, A. P.; Rothwell, I. P.; Huffman, J. C. *J. Am. Chem. Soc.* **1987**, *109*, 6471. Roskamp, E. J.; Pedersen, S. F. *J. Am. Chem. Soc.* **1987**, *109*, 6551. Roskamp, E. J.; Dragovich, P. S.; Hartung, J. B.; Pedersen, S. F. *J. Org. Chem.* **1989**, *54*, 4736. Yasuda, H.; Tatsumi, K.; Okamoto, T.; Mashima, K.; Lee, K.; Nakamura, A.; Kai, Y.; Kanahisa, N.; Kasai, N. *J. Am. Chem. Soc.* **1985**, *107*, 2410. Okamoto, T.; Yasuda, H.; Nakamura, A.; Kai, Y.; Kanahisa, N.; Kasai, N. *J. Am. Chem. Soc.* **1988**, *110*, 5008. Antinolo, A.; Carrillo, F.; Garcia-Yuste, S.; Otero, A. *Organometallics* **1994**, *13*, 2761.

(2) De Angelis, S.; Solari, E.; Gallo, E.; Floriani, C.; Chiesi-Villa, A.; Rizzoli, C. *Inorg. Chem.* **1992**, *31*, 2520. Giannini, L.; Solari, E.; De Angelis, S.; Ward, R. D.; Floriani, C.; Chiesi-Villa, A.; Rizzoli, C. *J. Am. Chem. Soc.* **1995**, *117*, 8501 and references therein.

(3) The organometallic chemistry of niobium based on porphyrinic skeleton had a very limited success: Green, M. H.; Moreau, J. J. E. *Inorg. Nucl. Chem. Lett.* **1972**, *8*, 1073.

(4) A publication on the organometallic derivatization of such complexes (Floriani, C.; Mazzanti, M.; Ciurli, S.; Chiesi-Villa, A.; Rizzoli, C. *J. Chem. Soc., Dalton Trans.* **1988**, 1361) is in preparation.

(5) (a) Jacoby, D.; Floriani, C.; Chiesi-Villa, A.; Rizzoli, C. *J. Am. Chem. Soc.* **1993**, *115*, 3595. (b) Jacoby, D.; Floriani, C.; Chiesi-Villa, A.; Rizzoli, C. *J. Am. Chem. Soc.* **1993**, *115*, 7025. (c) Jacoby, D.; Isoz, S. Floriani, C.; Chiesi-Villa, A.; Rizzoli, C. *J. Am. Chem. Soc.* **1995**, *117*, 2793. (d) Jacoby, D.; Isoz, S.; Floriani, C.; Chiesi-Villa, A.; Rizzoli, C. *J. Am. Chem. Soc.* **1995**, *117*, 2805.

(6) Solari, E.; Musso, F.; Floriani, C.; Chiesi-Villa, A.; Rizzoli, C. *J. Chem. Soc., Dalton Trans.* **1994**, 2015.

(7) De Angelis, S. Solari, E.; Floriani, C.; Chiesi-Villa, A.; Rizzoli, C. *J. Chem. Soc., Dalton Trans.* **1994**, 2467.

0276-7333/96/2315-0337$12.00/0

Table 1. Experimental Data for the X-ray Diffraction Studies on Crystalline Compounds 3, 4, 6, and 9

	3	4	6	9
formula	$C_{40}H_{56}F_3N_4NbO_4S\cdot C_4H_8O$	$C_{37}H_{51}N_4Nb$	$C_{47}H_{69}N_6Nb$	$C_{50}H_{74}LiN_4NbO_4\cdot 0.5C_4H_8O$
a, Å	11.820(3)	12.275(9)	19.423(3)	43.080(7)
b, Å	19.171(4)	12.728(5)	11.091(2)	11.988(7)
c, Å	10.994(3)	21.465(4)	20.805(3)	20.474(7)
α, deg	105.27(3)	90	90	90
β, deg	109.36(3)	96.40(3)	90.29(2)	103.26(2)
γ, deg	87.88(2)	90	90	90
V, Å^3	2263.9(11)	3333(3)	4481.8(13)	10292(7)
Z	2	4	4	8
fw	923.0	644.7	811.0	931.1
space group	*P*$\bar{1}$ (No. 2)	$P2_1/n$ (No. 14)	$P2_1/c$ (No. 14)	$C2/c$ (No. 15)
t, °C	22	22	22	22
λ, Å	0.71069	0.710 69	0.710 69	0.710 69
ρ_{calc}, g cm^{-3}	1.354	1.285	1.203	1.202
μ, cm^{-1}	3.56	3.74	2.92	2.67
transm coeff	0.938−1.000	0.690−1.000	0.780−1.000	0.982−1.000
R^a	0.041	0.063	0.072	0.075
w$R2^b$	0.102	0.169	0.156	0.203
GOF^c	1.008	1.102	1.082	1.177

^{a} $R = \sum||\Delta F|/\sum|F_o|$. ^{b} $wR2 = [\sum(w(\Delta F^2)^2/\sum(wF_o^2)^2]^{1/2}$. ^{c} GOF $= [\sum w|\Delta F|^2/(NO - NV)]^{1/2}$.

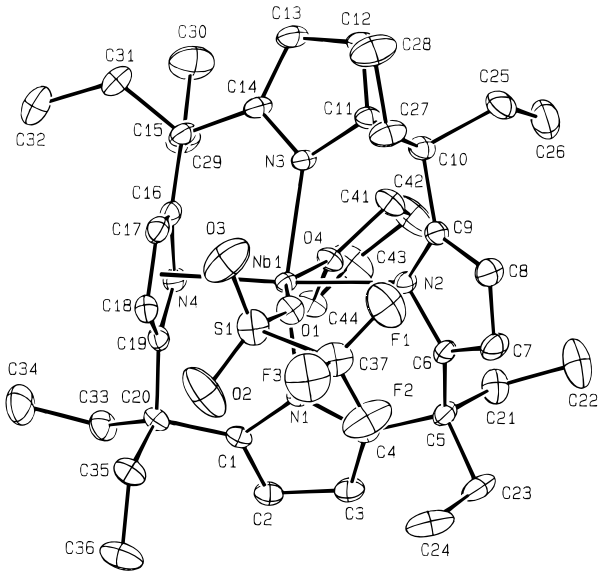

Figure 1. ORTEP drawing of complex **3** (30% probability ellipsoids).

respectively, to the metal. Thus the porphyrinogen tetraanion can provide between 8 and 24 electrons to the metal center. Also interesting are (ii) the stabilization of high metal oxidation states *via* a very peculiar redox system[8] and (iii) the bifunctionality of the derived metal−porphyrinogen complexes, where the metal acts as a Lewis acid center, while the electron-rich periphery can bind metal ions, in particular, alkali cations.[5]

We report here some unique examples of Nb−C σ bonds, having niobium(V) bonded to the porphyrinogen anion **I**. This includes the synthesis of the starting materials, niobium−porphyrinogen complexes, and their organometallic functionalized derivatives. A brief description of the synthesis of **4** and its reaction with carbon monoxide has been reported in the context of porphyrinogen homologation.[5c]

Results and Discussion

Contrary to other early transition metals in their highest oxidation states (molybdenum(VI),[9] tungsten(VI),[9] and vanadium(V)[9]) niobium(V) does not undergo reduction when reacted with the porphyrinogen tetraanion. The metalation of *meso*-octaethylporphyrinogen with $NbCl_5$ has been carried out by following conventional procedures used for other metals.[5−7]

Reaction of $[Et_8N_4Li_4(THF)_4]$, **1**,[7] with $NbCl_5$ in toluene led to the isolation of **2** in good yield (eq 1).

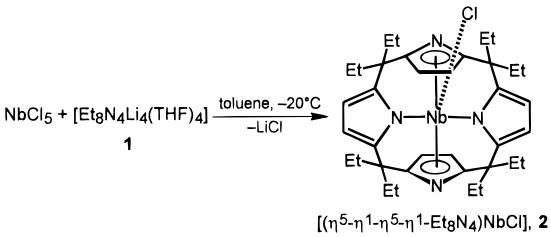

[$(\eta^5$-η^1-η^5-η^1-$Et_8N_4)NbCl$], **2**

The solid state structure we propose for **2** is essentially based on that of the isoelectronic [$(\eta^5$:η^1:η^5:η^1-$Et_8N_4)Zr(THF)$] complex,[5a] where the porphyrinogen skeleton displays the η^5:η^1:η^5:η^1 bonding mode for an electron-poor d^0 metal. Further support for this structure comes from the ^{1}H NMR spectrum, which shows a singlet at room temperature and two singlets at 243 K for the 3,4-protons of the pyrrole rings. This is in agreement with the fluxional behavior of the pyrrole fragments changing their bonding mode from η^1 to η^5, and we presume that the ^{1}H NMR spectrum at the lower temperature is closer to the solid state structure. An identical behavior has been observed for the zirconium analogue [$(\eta^5$:η^1:η^5:η^1-$Et_8N_4)Zr(THF)$].[5a]

Complex **2** should be considered as the starting material for lower oxidation states of niobium−porphyrinogen complexes and for the organometallic functionalization. In addition, the role of niobium(V) as a Lewis acid in a bifunctional structure can be particularly interesting for the activation of polar or ion-pair substrates. To this purpose, in order to increase the acidity at the metal center we produced the ionized form **3** (eq 2).

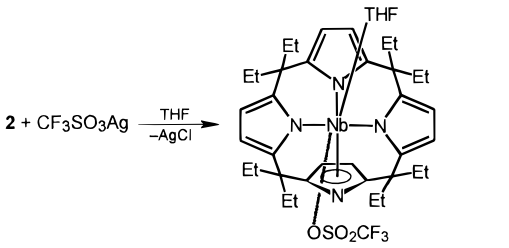

[$(\eta^5$-η^1-η^1-η^1-$Et_8N_4)Nb(OSO_2CF_3)(THF)$], **3**

(8) (a) De Angelis, S. Solari, E.; Floriani, C.; Chiesi-Villa, A.; Rizzoli, C. *J. Am. Chem. Soc.* **1994**, *116*, 5691. (b) Reference 8a, p 5702.

(9) Piarulli, U.; Floriani, C.; Chiesi-Villa, A.; Rizzoli, C. Manuscript in preparation.

Table 2. Selected Bond Distances (Å) and Angles (deg) for Complex 3[a]

Nb1−O1	2.111(2)	N3−C14	1.421(3)
Nb1−O4	2.301(2)	N4−C16	1.370(4)
Nb1−N1	2.125(3)	N4−C19	1.386(3)
Nb1−N2	2.111(2)	C1−C2	1.365(5)
Nb1−N3	2.150(3)	C2−C3	1.419(6)
Nb1−N4	2.391(2)	C3−C4	1.363(5)
Nb1−C16	2.437(3)	C6−C7	1.364(5)
Nb1−C17	2.516(4)	C7−C8	1.415(6)
Nb1−C18	2.589(4)	C8−C9	1.365(4)
Nb1−C19	2.470(3)	C11−C12	1.375(4)
Nb1−Cp4	2.179(4)	C12−C13	1.431(5)
N1−C1	1.424(5)	C13−C14	1.357(5)
N1−C4	1.406(4)	C16−C17	1.408(4)
N2−C6	1.421(3)	C17−C18	1.406(6)
N2−C9	1.423(5)	C18−C19	1.408(5)
N3−C11	1.397(5)		
N2−Nb1−N3	81.8(1)	Nb1−N1−C1	123.2(2)
N1−Nb1−N3	157.1(1)	C1−N1−C4	104.8(2)
N1−Nb1−N2	87.0(1)	Nb1−N2−C9	119.9(2)
Cp4−Nb1−N3	94.5(1)	Nb1−N2−C6	120.3(2)
Cp4−Nb1−N2	174.5(1)	C6−N2−C9	105.1(3)
Cp4−Nb1−N1	97.9(1)	Nb1−N3−C14	122.7(2)
O1−Nb1−O4	158.1(1)	Nb1−N3−C11	129.6(2)
Nb1−N1−C4	128.0(2)	C11−N3−C14	105.7(2)

[a] Cp4 refers to the centroid of the pyrrole ring containing N4.

Table 3. Selected Bond Distances (Å) and Angles (deg) for Complex 4[a]

Nb1−N1	2.126(6)	N3−C14	1.411(10)
Nb1−N2	2.153(6)	N4−C16	1.366(10)
Nb1−N3	2.140(7)	N4−C19	1.371(10)
Nb1−N4	2.330(6)	C1−C2	1.366(13)
Nb1−C16	2.413(6)	C2−C3	1.418(13)
Nb1−C17	2.537(9)	C3−C4	1.357(13)
Nb1−C18	2.532(9)	C6−C7	1.365(14)
Nb1−C19	2.446(7)	C7−C8	1.392(16)
Nb1−Cp4	2.151(6)	C8−C9	1.363(13)
Nb1−C37	2.162(9)	C11−C12	1.361(13)
N1−C1	1.402(11)	C12−C13	1.409(14)
N1−C4	1.410(11)	C13−C14	1.351(12)
N2−C6	1.423(10)	C16−C17	1.410(12)
N2−C9	1.383(11)	C17−C18	1.387(12)
N3−C11	1.392(12)	C18−C19	1.395(12)
N2−Nb1−N3	81.1(3)	C1−N1−C4	105.5(7)
N1−Nb1−N3	138.5(3)	Nb1−N2−C9	115.4(5)
N1−Nb1−N2	82.0(2)	Nb1−N2−C6	113.7(5)
Cp4−Nb1−N3	97.4(2)	C6−N2−C9	105.8(6)
Cp4−Nb1−N2	175.5(3)	Nb1−N3−C14	122.6(5)
Cp4−Nb1−N1	96.6(2)	Nb1−N3−C11	128.3(5)
Nb1−N1−C4	126.4(5)	C11−N3−C14	105.1(6)
Nb1−N1−C1	122.8(5)		

[a] Cp4 refers to the centroid of the pyrrole ring containing N4.

The increase in metal acidity of **3** *vs* that of **2** is reflected by the coordination of a THF molecule. The triflate anion is, usually, only weakly bonded and can be easily displaced by an incoming substrate. A question often raised in metal−porphyrinogen chemistry concerns the structural relationship between the solid state and that in solution. The structure shown above (eq 2) is based on the X-ray analysis. The variable-temperature ^{1}H NMR spectrum of **3** (toluene-d_8) shows changes in the 3,4-protons of the pyrrole ring, consistent with a change in bonding mode. At 333 K a well-resolved singlet is observed, in agreement with a fast fluxional behavior of the pyrrolyl anions. Cooling to 273 K results in two large singlets of equal intensity, which are in agreement either with a η^5:η^1:η^5:η^1 or a η^5:η^1:η^1:η^1 bonding mode, the later one having the two *trans* rings interconverting. At lower temperatures, however, the ^{1}H NMR spectrum approaches the solid state structure showing the pyrrolyl protons in 1:3 ratio (213 K), in agreement with the η^5:η^1:η^1:η^1 bonding mode of the porphyrinogen.

Table 4. Selected Bond Distances (Å) and Angles (deg) for Complex 6[a]

Nb1−N1	2.274(8)	N4−C19	1.368(15)
Nb1−N2	2.154(8)	N5−C38	1.243(13)
Nb1−N3	2.251(8)	N5−C39	1.490(14)
Nb1−N4	2.434(8)	N6−C43	1.141(14)
Nb1−N5	2.211(9)	N6−C44	1.476(16)
Nb1−C16	2.454(10)	C1−C2	1.380(18)
Nb1−C17	2.493(10)	C2−C3	1.354(22)
Nb1−C18	2.474(10)	C3−C4	1.379(18)
Nb1−C19	2.458(10)	C6−C7	1.370(16)
Nb1−Cp4	2.165(10)	C7−C8	1.388(19)
Nb1−C38	2.137(9)	C8−C9	1.388(16)
Nb1−C43	2.298(11)	C11−C12	1.371(15)
N1−C1	1.410(14)	C12−C13	1.398(17)
N1−C4	1.384(14)	C13−C14	1.381(15)
N2−C6	1.422(13)	C16−C17	1.394(15)
N2−C9	1.391(14)	C17−C18	1.407(15)
N3−C11	1.372(13)	C18−C19	1.382(15)
N3−C14	1.386(12)	C37−C38	1.510(13)
N4−C16	1.350(15)	C39−C42	1.554(18)
C38−Nb1−C43	148.9(4)	C1−N1−C4	106.8(8)
N5−Nb1−C43	157.9(3)	Nb1−N2−C9	120.5(6)
N2−Nb1−N3	83.7(3)	Nb1−N2−C6	119.8(6)
N1−Nb1−N3	153.4(3)	C6−N2−C9	105.1(7)
N1−Nb1−N2	82.5(3)	Nb1−N3−C14	122.3(6)
Cp4−Nb1−N3	97.0(4)	Nb1−N3−C11	130.4(6)
Cp4−Nb1−N2	177.0(4)	C11−N3−C14	106.4(8)
Cp4−Nb1−N1	95.6(4)	C38−N5−C39	132.1(9)
Nb1−N1−C4	129.5(7)	N5−C38−C37	136.2(10)
Nb1−N1−C1	122.0(6)		

[a] Cp4 refers to the centroid of the pyrrole ring containing N4.

Table 5. Selected Bond Distances (Å) and Angles (deg) for Complex 9

Nb1−O1	1.741(7)	C1−C2	1.368(15)
Nb1−N1	2.124(8)	C2−C3	1.408(19)
Nb1−N2	2.158(9)	C3−C4	1.371(16)
Nb1−N3	2.170(9)	C6−C7	1.373(17)
Nb1−N4	2.436(8)	C7−C8	1.365(20)
Nb1−C30	2.242(8)	C8−C9	1.377(17)
N1−C1	1.399(14)	C11−C12	1.375(15)
N1−C4	1.396(12)	C12−C13	1.400(21)
N2−C6	1.400(13)	C13−C14	1.367(16)
N2−C9	1.374(14)	C16−C17	1.378(15)
N3−C11	1.388(15)	C17−C18	1.388(15)
N3−C14	1.398(13)	C18−C19	1.363(15)
N4−C16	1.359(11)	C18−C34	1.552(18)
N4−C20	1.363(12)	C19−C20	1.376(16)
N −Nb1−N4	83.9(3)	Nb1−N2 −C6	118.0(7)
N2−Nb1−N4	133.8(3)	C6−N2 −C9	106.5(8)
N2−Nb1−N3	78.7(3)	Nb1−N3 −C14	117.2(6)
N1−Nb1−N4	78.9(3)	Nb1−N3 −C11	137.6(7)
N1−Nb1−N3	137.1(3)	C11−N3 −C14	105.1(8)
N1−Nb1−N2	85.5(3)	Nb1−N4 −C20	130.2(6)
O1−Nb1−C30	81.7(3)	Nb1−N4 −C16	111.5(6)
N1−Nb1−N3	137.1(3)	C16−N4 −C20	117.4(7)
Nb1−N1−C4	113.8(6)	Nb1−C30−C15	107.6(6)
Nb1−N1−C1	126.9(6)	C15−C30−C31	116.5(8)
C1−N1−C4	106.6(8)	Nb1−C30−C31	110.0(6)
Nb1−N2 −C9	135.0(7)		

The structure consists of discrete **3** units (Figure 1) and THF solvent molecules of crystallization in the complex/solvent molar ratio of 1/1. Table 2 gives selected bond distances and angles. The relevant conformational parameters are given in Table 6. Throughout the text the pyrrole rings containing the N1, N2, N3, and N4 nitrogen atoms will be indicated as A, B, C, and D, respectively. The porphyrinogen ligand exhibits a η^5:η^1:η^1:η^1-bonding mode with the η^5-bonded pyrrole ring (D) nearly perpendicular to the N_4 core [dihedral angle 102.1(1)°]. A small but significant tetrahedral distortion is observed in the N_4 core, the

Table 6. Comparison of Structural Parameters for Compounds 3, 4, 6, and 9

		3	4	6	9[a]
dist of atoms from N4 core, Å	N1	−0.046(2)	−0.035(6)	−0.063(8)	−0.050(8)
	N2	0.050(2)	0.039(1)	0.054(7)	0.064(9)
	N3	−0.044(2)	−0.052(8)	−0.064(8)	−0.061(9)
	N4	0.040(2)	0.033(6)	0.063(9)	0.053(8)
	Nb	0.454(1)	0.708(1)	0.568(1)	0.839(2)
dist of Nb from A, Å		0.695(1)	0.829(1)	0.441(1)	1.175(1)
dist of Nb from B, Å		1.252(1)	1.645(1)	1.342(1)	0.313(1)
dist of Nb from C, Å		0.449(1)	0.782(1)	0.346(1)	0.168(1)
dist of Nb from D, Å		2.168(1)	2.141(1)	2.163(1)	0.626(1)
dihedral angles between the N4 core and the A−D rings, deg	(A)	145.8(1)	137.0(2)	175.0(4)	161.7(3)
	(B)	154.8(1)	148.9(2)	158.6(3)	155.9(3)
	(C)	155.2(1)	138.2(2)	170.2(3)	145.4(3)
	(D)	102.1(1)	97.8(3)	102.9(3)	139.3(3)
dist of nitrogen atoms from the plane of the bonded atoms, Å	N1	0.185(2)	0.211(6)	0.118(8)	0.329(8)
	N2	0.359(2)	0.470(6)	0.358(7)	0.068(9)
	N3	0.127(2)	0.184(7)	0.089(8)	0.041(9)
	N4	0.087(8)			

[a] A−D refer to the pyrrole rings containing N1−N4, respectively. For complex **9** D refers to the pyridine ring.

niobium atom being displaced by 0.454(1) Å toward the O1 oxygen atom of the $CF_3SO_3^-$ anion. Coordination around niobium (distorted octahedron) is completed by an oxygen atom (O4) from a THF molecule. The dihedral angles formed by the direction of the Nb−O lines with the normal to the N_4 core are 26.1(1) and 4.2(1)° for Nb−O1 and Nb−O4, respectively. The Nb−N σ-bond distances [Nb−N1, 2.125(3), Nb−N2, 2.111(2), Nb−N3, 2.150(3) Å] are very close each other and are in agreement with those found in complexes **4** and **9**. The η^5 bonding mode of the D ring is evidenced by the narrow range of the niobium−nitrogen and niobium−carbon distances (Table 2). There is a remarkable difference between the Nb−O bond distances [Nb−O1, 2.111(2), Nb−O4, 2.301(2) Å], the shortest one involving the charged ligand. The [(Et_8N_4)Nb] moiety assumes a double saddle shape conformation, the four pyrrole rings being tilted up and down alternatively with respect to the N_4 core (Table 6). The trend of the N−C and C−C bonds in the η^5-bonded pyrrole rings is consistent with a partial double bond localization on the C−C distances adjacent to the macrocycle [1.366(3) Å is the mean value averaged on the bond distances C1−C2, C3−C4, C6−C7, C8−C9, C11−C12, C13−C14; 1.417(4) Å is the mean value averaged on the N−C bond distances; 1.423(5) Å is the mean value averaged on the bond distances C2−C3, C7−C8, C12−C13], while in the bonded D ring they are consistent with a π delocalization [mean N−C bond distance, 1.380(8) Å; mean C−C bond distance, 1.408(6) Å]. This is in agreement with the pyramidal geometry of the Nb−η^1-bonded nitrogen atoms (Table 6).

The use of **1** as starting material for an organometallic derivatization is shown in eq 2. The alkylation of **2** was carried out in toluene using LiMe to give the methyl derivative **4** (eq 3).

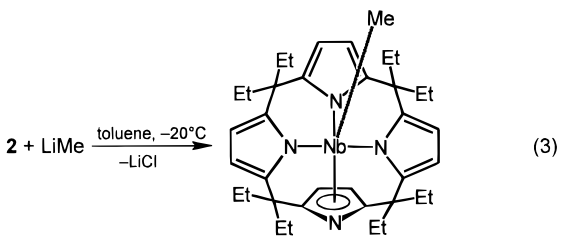

[(η^5-η^1-η^1-η^1-Et_8N_4)Nb–Me], **4**

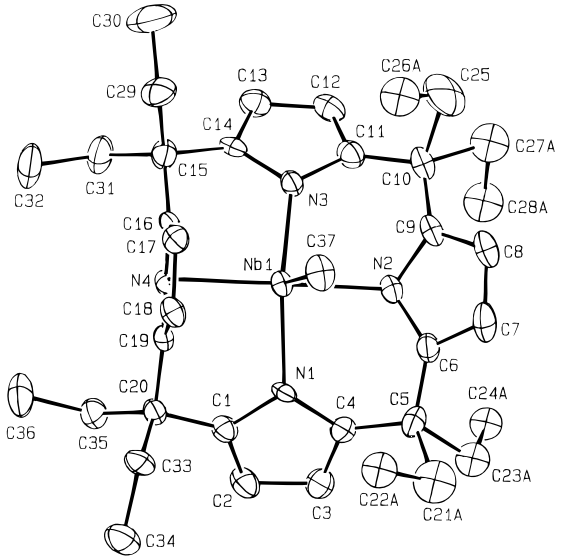

Figure 2. ORTEP drawing of complex **4** (30% probability ellipsoids). The disorder is omitted for clarity.

The structure indicated is that observed in the solid state, as determined by an X-ray analysis (*vide infra*). However, in solution at room temperature complex **3** shows the pyrrolic protons as two singlets of equal intensity, which are in agreement either with a η^5:η^1:η^5:η^1 or a η^5:η^1:η^1:η^1 bonding mode, the later one having the two *trans* rings interconverting. At lower temperatures, however, the ^{1}H NMR spectrum approaches the solid state structure showing the pyrrolyl protons in 1:3 ratio (223 K), in agreement with the η^5:η^1:η^1:η^1 bonding mode of the porphyrinogen.

The [(Et_8N_4)Nb] moiety (Figure 2) has a conformation similar to that observed in complex **3** (Table 6). The niobium atom is strongly displaced [0.708(1) Å] from the mean N_4 plane toward the methyl carbon. The N_4 core shows small but significant tetrahedral distortions from planarity (Table 6). The η^1-bonded pyrrole rings are midway between being parallel and perpendicular to that plane (Table 6), while the η^5-bonded D ring is nearly perpendicular. In particular the A and C pyrrole rings are oriented downward, while the others are tilted upward with respect to the fifth coordination site giving rise to the usually observed double saddle shape conformation. The bonding mode of the macrocycle is very similar to that observed in **3**, as indicated by the values

of the corresponding bond distances and angles, except for the N1−Nb−N3 angle which reflects the different bending of the involved pyrrole rings with respect to the N_4 core and the different displacement of the metal atom from that plane. This could be a consequence of the different coordination number of niobium in the two complexes. The Nb−C37 bond distance [2.174(9) Å] is in agreement with the values quoted in the literature for niobium−carbon σ bonds.[1] Bond distances and angles within the pyrrole rings show the trend observed in complex **3** [1.360(5) Å is the mean value averaged on the bond distances C1−C2, C3−C4, C6−C7, C8−C9, C11−C12, C13−C14; 1.405(6) Å is the mean value averaged on the N−C bond distances; 1.408(7) Å is the mean value averaged on the bond distances C2−C3, C7−C8, C12−C13], while in the η^5-bonded D ring they are consistent with a π delocalization [mean N−C bond distance, 1.369(3) Å; mean C−C bond distance, 1.397(7) Å]. This is consistent with the pyramidal geometry of the Nb−η^1-bonded nitrogen atoms (Table 6).

The migratory aptitude of the methyl group in complex **4** was demonstrated in its reaction with Bu^{t}NC.[10,11] This should simulate the preliminary, undetectable step of the reaction of **3** with carbon monoxide which leads to the homologation of a pyrrole ring.[5c] Rare examples of the migratory insertion of RNC into a Nb−C bond[12] or of the obtention of iminoacyls by other routes[13] have been reported. Reaction 4 seems to proceed *via* two well

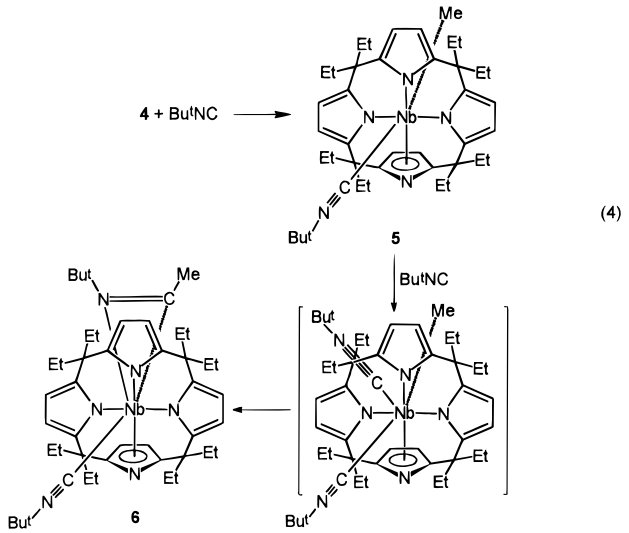

(4)

distinct steps. The first one corresponds to the coordination of the isocyanide *trans* to the methyl group and should labilize the methyl group. The second one corresponds to the coordination of a second isocyanide molecule *cis* to the methyl and is followed by the formation of the η^2-iminoacyl functionality. This is consistent with the following experimental evidence: when the reaction is carried out with a ButNC:Nb = 1:1 molar ratio, a mixtures of **4**−**6** are obtained, while the use of a 2:1 ratio results exclusively in **6**. This supports the preliminary formation of **5**, which should be a *trans* isomer, followed by a fast *cis* insertion of isocyanide into the Nb−Me bond. Pure **5** could not be isolated, but in the case of the 1:1 ratio, **5** was obtained as a crystalline solid mixed with **6** (see the Experimental Section).

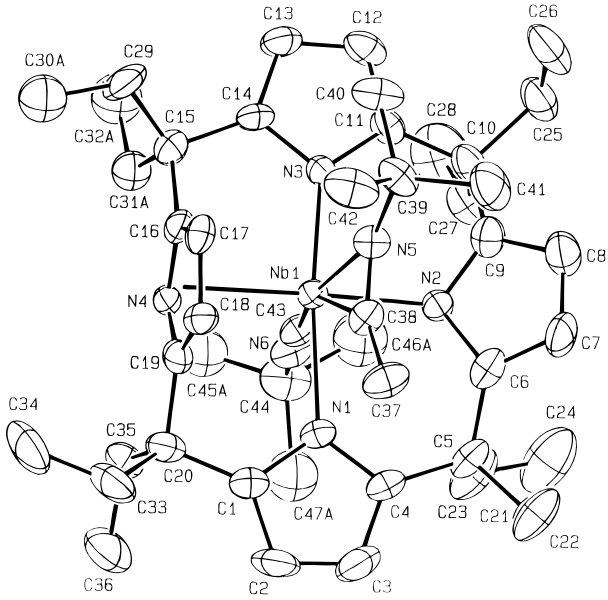

Figure 3. ORTEP drawing of complex **6** (30% probability ellipsoids). The disorder is omitted for clarity.

The porphyrinogen bonding mode shown for **6** is that observed in the solid state, not necessarily that in solution. Unfortunately the ^{1}H NMR data are not much informative for two factors. First, there is the usual fluxional behavior between the η^1- and the η^5-bonding modes of the pyrrolyl anions, while the second problem arises from the inequivalence of the pyrrolyl anions introduced by the η^2-iminoacetyl ligand. The IR spectrum is diagnostic for the presence of Bu^{t}NC (2217 cm^{-1}) and iminoacetyl (1736 cm^{-1}) groups.

The solid state structure of **6** is shown in Figure 3. The out-of-plane distance of Nb from the N_4 core [0.568(1) Å] is significantly smaller than that in **4**, Nb remaining still displaced toward the charged ligand (Table 6). Selected bond distances and angles are listed in Table 4. The orientation of the pyrrole rings in the [(Et_8N_4)Nb] moiety (Figure 3) is remarkably different from those present in complexes **3** and **4**, in spite of the same η^1:η^1:η^1:η^5-bonding mode exhibited by porphyrinogen. This could be a consequence of the six coordination number of niobium involving sterically bulky ligands. Indeed the more remarkable difference concerns the orientation of the two opposite A and C σ-bonded rings which in **6** are nearly parallel to the N_4 coordination

(10) (a) Durfee, L. D.; Rothwell, I. P. *Chem. Rev.* **1988**, *88*, 1059. (b) Wolczanski, P. T.; Bercaw, J. E. *Acc. Chem. Res.* **1980**, *13*, 121. (c) Headford, C. E. L.; Roper, W. R. In *Reactions of Coordinated Ligands*; Braterman, P. S., Ed.; Plenum: New York, 1986; Vol. 1, Chapter 8. (d) Carlin, D. J.; Lappert, M. F.; Raston, C. L. *Chemistry of Organo-Zirconium and -Hafnium Compounds*; Ellis Horwood: Chichester, U.K., 1986. (e) Labinger, J. A. *Transition Metal Hydrides*; Dedieu, A., Ed.; VCH: Weinheim, Germany, 1992.

(11) (a) Singleton, E.; Ossthnizen, H. E. *Adv. Organomet. Chem.* **1983**, *22*, 209. (b) Otsuka, S.; Nakamura, A.; Yoshida, T.; Naruto, M.; Ataba, K. *J. Am. Chem. Soc.* **1973**, *95*, 3180. (c) Yamamoto, Y.; Yamazaki, H. *Inorg. Chem.* **1974**, *13*, 438. (d) Aoki, K.; Yamamoto, Y. *Inorg. Chem.* **1976**, *15*, 48. (e) Bellachioma, G.; Cardaci, G.; Zanazzi, P. *Inorg. Chem.* **1987**, *26*, 84. (f) Maitlis, P. M.; Espinet, P.; Russell, M. J. H. In *Comprehensive Organometallic Chemistry*; Wilkinson, G., Stone, F. G. A., Abel, E. W., Eds.; Pergamon: London, 1982; Vol. 8, Chapter 38.4. (g) Crociani, B. In *Reactions of Coordinated Ligands*; Braterman, P. S., Ed.; Plenum: New York, 1986; Chapter 9. (h) Ruiz, J.; Vivanco, M.; Floriani, C.; Chiesi-Villa, A.; Rizzoli, C. *Organometallics* **1993**, *12*, 1811. (i) Klose, A.; Solari, E.; Ferguson, R.; Chiesi-Villa, A.; Rizzoli, C. *Organometallics* **1993**, *12*, 2414.

(12) Hirpo, W.; Curtis, M. D. *Organometallics* **1994**, *13*, 2706.

(13) Martinez de Ilarduya, J. M.; Otero, A.; Royo, P. *J. Organomet. Chem.* **1988**, *340*, 187. Antinolo, A.; Fajardo, M.; Lopez-Mardomingo, C.; Martin-Villa, P.; Otero, A. *Organometallics* **1991**, *10*, 3435. Antinolo, A.; Fajardo, M.; Gil-Sanz, R.; Lopez-Mardomingo, C.; Martin-Villa, P.; Otero, A.; Kubicki, M. M.; Mugnier, Y.; El Krami, S.; Mourad, Y. *Organometallics* **1993**, *12*, 381.

plane as to make room for the approaching of the sixth ligand. The η^5-bonded pyrrole ring (D) is nearly perpendicular to the N_4 plane (Table 6). A similar trend, though to a lesser extent, has been observed in six-coordinate **3** with respect to five-coordinate **4.** As a probable consequence, the Nb−N1 [2.274(8) Å] and Nb−N3 [2.251(8) Å] bond distances are significantly longer than the Nb−N2 bond distance [2.154(8) Å], which is in agreement with the values found in complexes **3**, **4**, and **9** for η^1-bonded pyrrole rings. The iminoacyl group is slightly asymmetrically η^2-bonded to the metal [Nb−N5, 2.211(9), Nb−C38, 2.137(9) Å]. The plane through the metal atom and the η^2-bonded iminoacyl group forms a dihedral angle of 66.6(2)° with the N_4 core which shows the most remarkable tetrahedral distortions. The Nb−C bond distances are very close in **4** and **6** [Nb−C37, 2.162(9) Å, **4**; Nb−C38, 2.137(9) Å, **6**], which implies a very low carbenoid nature of the iminoacyl and is further supported by a short C═N distance [1.250(14) Å] and rather high C═N stretching frequency [1736 cm^{-1}].

Organometallic functionalization of a metal center is usually made using a metathesis reaction with the metal−halide bond. Another reaction which has scarcely been considered in that context is the ketonic-like M═O oxo functionality.[14] Its reactivity with an alkylating agent should, in principle, parallel the addition of a Grignard to a ketone. Our model compound is the niobyl derivative **7**, which has been synthesized directly from the reaction of **4** with carbon monoxide.[5c]

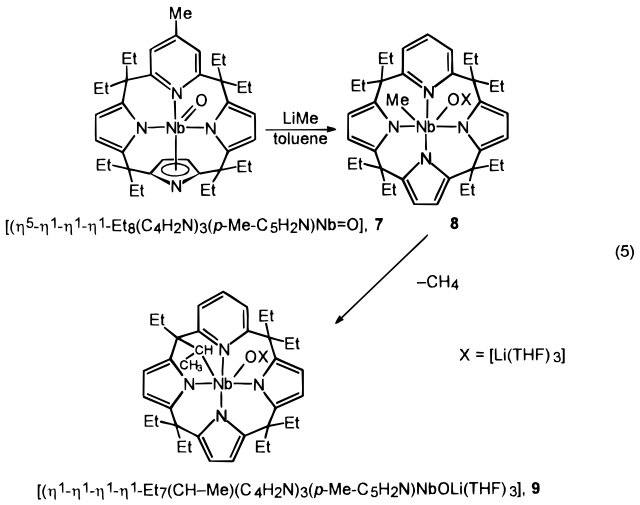

The reaction was carried out at −18 °C by adding LiMe to a toluene solution of **7**. The addition of LiMe to the Nb═O should lead to the intermediate **8**, as expected from a ketone-like reactivity of the Nb═O functionality. The close proximity of the Me group to one of the methylene groups of the *meso*-ethyls assists methane elimination and metalation of the *meso*-substituents. A significant support to such a mechanism comes from the observation that $LiBu^n$, which is a much better deprotonating, but a worse alkylating, agent than LiMe, is almost inefficient in the same reaction. The metal-assisted metalation of the peripheral ethyl chains has been observed in the reaction of the zirconium−*meso*-octaethylporphyrinogen complex with a large excess of metal hydrides.[5d]

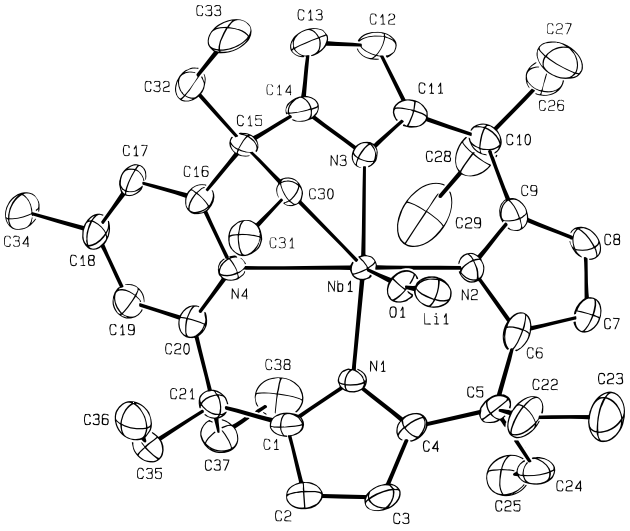

Figure 4. ORTEP drawing of complex **9** (30% probability ellipsoids). The THF molecules bonded to Li^+ have been omitted for clarity.

Although the NMR spectra are quite diagnostic of the structure of **9**, the best answer on the structural details comes from an X-ray analysis.

The structure of **9** is shown in Figure 4. Coordination around niobium assumes a distorted bicapped pyramid, with the four nitrogen atoms defining the basal plane and the O1 oxo oxygen and the C30 carbon at the apices. The N_4 core shows significant tetrahedral distortions, the niobium being displaced by 0.839(2) Å toward the *cis* coordinated atoms. The plane through Nb1, O1, and C30 is nearly perpendicular to the N_4 core, the dihedral angle being 93.2(3)°. The directions of the Nb−O1 and Nb−C30 lines are tilted by 24.2(3) and 57.8(3)°, respectively, with respect to the normal to the N_4 mean plane. Metalation strongly influences the conformation of the porphyrinogen ligand with respect to that of the starting complex **7**, imposing a η^1:η^1:η^1-η^1 bonding mode, probably as a consequence of a reduced electronic demand of the metal. The Nb−N(pyrrole) bond distances are comparable with those observed in **4** and **6**. The Nb−N4 bond distance involving the pyridine ring [2.436(8) Å] is remarkably longer than the Nb−N(pyrrole) bond distances. It is just significantly longer than that found in **6** [2.404(6) Å, mean value], where the metal exhibits pyramidal coordination, as well as the Nb−O1 bond distance [1.741(7) *vs* 1.708(4) Å, mean value]. The steric factors may be responsible for a rather long Nb−C30 bond distance [2.242(8) Å].

Experimental Section

General Procedure. All reactions were carried out under an atmosphere of purified nitrogen. Solvents were dried and distilled before use by standard methods. The synthesis of complex **1** was carried out as reported.[5a,7] Infrared spectra were recorded with a Perkin-Elmer 883 spectrophotometer; ^1H NMR spectra were measured on a 200-AC Bruker instrument.

Synthesis of 2. $NbCl_5$ (8.57 g, 31.71 mmol) was added to a toluene (300 mL) solution of **1** (27.12 g, 31.79 mmol) at −20 °C, and the reaction mixture was allowed to reach room temperature and left stirring overnight. The mixture was extracted with the mother liquor for 2 h, the solvent evaporated, and the residue treated with *n*-hexane (100 mL). A brown powder was obtained, which was filtered out and dried

(14) Housmekerides, C. E.; Ramage, D. L.; Kretz, C. M.; Shontz, J. T.; Pilato, R. S.; Geoffroy, G. L.; Rheingold, A. L.; Haggerty, B. S. *Inorg. Chem.* **1992**, *31*, 4453. Nugent, W. A.; Mayer, J. M. *Metal-Ligand Multiple Bonds*; Wiley: New York, 1988.

(70%). ^{1}H NMR (200 MHz, $C_6D_5CD_3$, room temperature): δ 0.91 (t, 12 H, J = 7.32 Hz, CH_3), 1.04 (t, 12 H, J = 7.34 Hz, CH_3), 2.0−2.2 (m, 16 H, CH_2), 6.34 (s, 8 H, CH). At lower temperature, two singlets are seen for the 3,4 pyrrolic protons: ^{1}H NMR (200 MHz, $C_6D_5CD_3$, 243 K) δ 6.18 (s, 4 H, CH), 6.54 (s, 4 H, CH). Anal. Calcd for $C_{36}H_{48}ClN_4Nb$: C, 64.99; H, 7.28; N, 8.43. Found: C, 64.99; H, 7.91; N, 8.32.

Synthesis of 3. A THF (75 mL) solution of **2** (2.40 g, 3.61 mmol) was treated with $AgOSO_2CF_3$ (0.93 g, 3.63 mmol) resulting in an immediate red color change. Solid AgCl formed on stirring for 3 h, which was then removed by filtration, and the resulting eluent was taken to dryness. The residue was washed with *n*-hexane (63%) and then recrystallized from a mixture of THF/*n*-hexane (30%). ^{1}H NMR (200 MHz, C_6D_6, room temperature): δ 0.73 (t, 12H, J = 7.36, CH_3); 0.84 (t, 12H, J = 7.32, CH_3); 1.15 (m, 4H, THF); 1.70 (m, 4H, THF); 1.7−2.1 (m, 16H, CH_2); 3.23 (m, 4H, THF); 3.30 (m, 4H, THF); 5.6−6.9 (m broad, 8H, CH). The following data are for the 3,4 pyrrolic protons (200 MHz, C_7D_8): 333 K, δ 6.31 (s, 8H, CH); 298 K, δ 6.0−6.7 (m broad, 8H, CH); 273 K, δ 5.90 (s, 4H, CH), 6.80 (s, 4H, CH); 213 K, δ 5.88 (s, 6H, CH), 7.50 (m, broad, 2H, CH). Anal. Calcd for $C_{45}H_{64}F_3N_4NbO_5S$: C, 58.55; H, 7.00; N, 6.07. Found: C, 58.46; H, 7.20; N, 6.28.

Synthesis of 4. Method A. MeLi (8.0 mL, 1.6 M in Et_2O, 12.80 mmol) was added dropwise to a toluene (200 mL) solution of **2** (22.07 g, 33.17 mmol) at −20 °C, and the reaction mixture was allowed to reach room temperature and then stirred overnight. The resulting green mixture was filtered to eliminate LiCl, the solvent evaporated to dryness, and the residue then collected with *n*-hexane (100 mL). A green microcrystalline solid was obtained, which was filtered out and dried (81%). Crystals suitable for X-ray analysis were grown in hexane/THF. ^{1}H NMR (200 MHz, $C_6D_5CD_3$, room temperature): δ 0.76 (s, CH_3−Nb, 3 H), 0.9−1.1 (m, CH_3, 24 H), 1.9−2.4 (m, CH_2, 16 H), 6.19 (s, CH, 4 H), 6.54 (s, CH, 4 H). The following data are for the 3,4 pyrrolic protons: 223 K, δ 6.30 (s, CH, 6 H), 6.66 (s, CH, 2 H). Anal. Calcd for $C_{37}H_{51}N_4$-Nb: C, 68.91; H, 7.98; N, 8.69. Found: C, 69.31; H, 8.23; N, 8.69.

Method B. $NbCl_5$ (2.21 g, 8.17 mmol) was added to a solution of **1** (7.00 g, 8.20 mmol) in toluene (75 mL). The suspension was stirred at room temperature for 15 h, and the resulting LiCl was removed by filtration. The eluant was then cooled to −30 °C to which LiMe (5.1 mL), 8.16 mmol) was added dropwise. The suspension was stirred for 15 h at room temperature, and again LiCl was removed by filtration. The solvent was evaporated to dryness and the residue washed with *n*-hexane (50 mL). The green microcrystalline solid was analyzed as such (79%).

Synthesis of 6. Bu^{t}NC (0.55 mL, 0.41 g, 4.89 mmol) was added to a toluene (50 mL) solution of **4** (1.27 g, 1.97 mmol) and the mixture stirred at 50 °C overnight. Toluene was evaporated from the reaction mixture, and the remaining residue was collected with *n*-hexane (40 mL), yielding a brown-orange powder (68%). Red crystals suitable for X-ray analysis were obtained by recrystallization in hexane/toluene. ^{1}H NMR (200 MHz, C_6D_6, room temperature): δ 0.83 (s, Bu^t, 9 H), 0.84 (t, CH_3, 12 H, J = 7.38 Hz), 0.93 (s, Bu^t, 9 H), 1.15 (t, CH_3, 12 H, J = 7.35 Hz), 2.06 (s, CH_3C=NBu^t, 3 H), 1.95−2.20 (m, CH_2, 16 H), 6.04 (s, CH, 8 H). IR: ν(N=C) 1736 and 2217 cm^{-1}. Anal. Calcd for $C_{42}H_{69}N_6Nb$: C, 69.59; H, 8.59; N, 10.36. Found: C, 69.60; H, 8.52; N, 10.08. When the reaction was carried out with Bu^{t}NC in a 1:1 molar ratio, a mixture of **5** and **6** was obtained. Bu^{t}NC (0.38 mL, 3.38 mmol) was added to a toluene (75 mL) solution of **4** (2.09 g, 3.25 mmol). The solution was stirred for 3 h and turned red-orange. Then the solvent was evaporated to dryness. The solid recrystallized from toluene/hexane gave a mixture of orange and brown crystals, **5** (30%). The crystals were separated under the microscope. The brown crystals have an IR spectrum with a single C=N band at 2217 cm^{-1}, while the orange crystals are complex **6**.

Synthesis of 9. A toluene (50 mL) solution of **6** (1.08 g, 1.61 mmol) was reacted with an Et_2O solution of LiMe (1.6 mmol). The orange color turned suddenly yellow-brown and then, after stirring overnight at room temperature, yellow-green. The yellow-green solid was collected and recrystallized from THF/hexane (78%). ^{1}H NMR (200 MHz, THF-d_8, room temperature): δ -0.21 (t, 3H, J = 7.21, CH_3CH−Nb), 0.15 (t, 3H, J = 6.92, CH_3), 0.21 (t, 3H, J = 7.34, CH_3), 0.40 (t, 3H, J = 7.16, CH_3), 0.57 (t, 3H, J = 7.05, CH_3), 0.9−1.1 (m, 9H, CH_3), 1.1-2.6 (m, 14H, CH_2), 2.22 (s, 3H, CH_3−py), 3.23 (q, 1H, CH−Nb), 5.47 (d, 1H, J = 3.09, CH pyrrole), 5.59 (d, 1H, J = 3.07, CH pyrrole), 5.74 (d, 1H, J = 3.25, CH pyrrole), 5.79 (d, 1H, J = 3.06, CH pyrrole), 5.99 (d, 1H, J = 3.33, CH pyrrole), 6.10 (d, 1H, J = 3.10, CH pyrrole), 6.92 (s, 1H, CH pyridine), 7.10 (s, 1H, CH pyridine). Anal. Calcd for $C_{50}H_{74}LiN_4NbO_4$: C, 67.09: H, 8.35; N, 6.26. Found: C, 67.67: H, 8.59; N, 6.26. IR: ν(C=NPy) 1558, 1616 cm^{-1}.

X-ray crystallography for Complexes 3, 4, 6, and 9. Suitable crystals were mounted in glass capillaries and sealed under nitrogen. The reduced cells were obtained with the use of TRACER.[15] Crystal data and details associated with data collection are given in Tables 1 and S1. Data were collected at room temperature (295 K) on a single-crystal diffractometer (Philips PW1100 for **3**, Rigaku AFC6S for **4** and **9**, and Siemens AED for **6**). For intensities and background individual reflection profiles were analyzed.[16] The structure amplitudes were obtained after the usual Lorentz and polarization corrections,[17] and the absolute scale was established by the Wilson method.[18] The crystal quality was tested by ψ scans showing that crystal absorption effects could not be neglected. The data were corrected for absorption using a semiempirical method[19] for complexes **3**, **4**, and **9** and ABSORB[20] for **6**. The function minimized during the least-squares refinement was $\sum w(\Delta F^2)^2$. Weights were applied according to the scheme $w = 1/[\sigma^2(F_o)^2 + (aP)^2]$ ($P = (F_o^2 + 2F_c^2)/3$) with a = 0.0635, 0.0937, 0.0446, and 0.0815 for complexes **3**, **4**, **6**, and **9**, respectively. Anomalous scattering corrections were included in all structure factor calculations.[21b] Scattering factors for neutral atoms were taken from ref 21a for non-hydrogen atoms and from ref 22 for H. Among the low-angle reflections no correction for secondary extinction was deemed necessary.

All calculations were carried out on an IBM PS2/80 personal computer and on an ENCORE 91 computer. The structures were solved by the heavy-atom method starting from three-dimensional Patterson maps using the observed reflections. Structure refinements were based on the unique observed data using SHELXL92.[23]

Refinement was first done isotropically and then anisotropically for all non-H atoms except for the disordered atoms. The THF molecules in complexes **3** and **9** and some ethyl and methyl groups in complexes **4**, **6**, and **9** were found to be affected by disorder, which was solved by considering the carbon atoms with higher thermal parameters as statistically distributed over two positions (A and B) isotropically refined with the site occupation factors given in Tables S2−S5. During the refinement the C−C bond distances involving the disordered atoms were constrained to be 1.54(1) Å. In the THF

(15) Lawton, S. L.; Jacobson, R. A. *TRACER (a cell reduction program)*; Ames Laboratory, Iowa State University of Science and Technology: Ames, IA, 1965.
(16) Lehmann, M .S.; Larsen, F. K. *Acta Crystallogr., Sect. A: Cryst. Phys., Diffr., Theor. Gen. Crystallogr.* **1974**, *A30*, 580−584.
(17) Data reduction was carried out on an IBM AT personal computer equipped with an INMOS T800 transputer.
(18) Wilson, A. J. C. *Nature* **1942**, *150*, 151.
(19) North, A. C. T.; Phillips, D. C.; Mathews, F. S. *Acta Crystallogr., Sect. A: Cryst. Phys., Diffr., Theor. Gen. Crystallogr.* **1968**, *A24*, 351.
(20) Ugozzoli, F. *Comput. Chem.* **1987**, *11*, 109.
(21) (a) *International Tables for X-ray Crystallography*; Kynoch Press: Birmingham, England, 1974; Vol. IV, p 99. (b) *Ibid.*, p 149.
(22) Stewart, R. F.; Davidson, E. R.; Simpson, W. T. *J. Chem. Phys.* **1965**, *42*, 3175.
(23) Sheldrick, G. M. *SHELXL92: Program for Crystal Structure Refinement*; University of Göttingen: Göttingen, Germany, 1992.

solvent molecules of crystallization in complexes **3** and **9** there was no possibility to distinguish between oxygen and carbon atoms.

The hydrogen atoms, except those related to disordered carbon atoms, which were ignored, were located from difference Fourier maps for **3**, **4**, and **6** and put in geometrically calculated positions for **9**. They were introduced in the subsequent refinements as fixed atom contribution with *U*'s fixed at 0.10 for **3**, **4**, and **9** and 0.12 Å^2 for **6**. The final difference maps showed no unusual feature, with no significant peak above the general background.

Final atomic coordinates are listed in Tables S2−S5 for non-H atoms and in Tables S6−S9 for hydrogens. Thermal parameters are given in Tables S10−S13, and bond distances and angles are in Tables S14−S17.[24]

Acknowledgment. We thank the "Fonds National Suisse de la Recherche Scientifique" (Grant No. 20-40268.94) and Ciba-Geigy SA (Basel, Switzerland) for financial support.

Supporting Information Available: Tables S1−S17, listing experimental details associated with data collection and structure refinement, final atomic coordinates for non-H atoms, hydrogen atom coordinates, thermal parameters, and bond distances and angles for **3**, **4**, **6**, and **9**, and SCHAKAL drawings for **3** and **4** (31 pages). Ordering information is given on any current masthead page.

OM950537Z

(24) See paragraph at the end of paper regarding Supporting Information.